

Single-top-quark production at hadron colliders

T. Stelzer, Z. Sullivan and S. Willenbrock

Department of Physics
University of Illinois
1110 West Green Street
Urbana, IL 61801

Abstract

Single-top-quark production probes the charged-current weak interaction of the top quark, and provides a direct measurement of the CKM matrix element V_{tb} . We perform two independent analyses to quantify the accuracy with which the W -gluon fusion ($gq \rightarrow t\bar{b}q$) and $q\bar{q} \rightarrow t\bar{b}$ signals can be extracted from the backgrounds at both the Tevatron and the LHC. Although perturbation theory breaks down at low transverse momentum for the W -gluon fusion \bar{b} differential cross section, we show how to obtain a reliable cross section integrated over low \bar{b} transverse momenta up to a cutoff. We estimate the accuracy with which V_{tb} can be measured in both analyses, including theoretical and statistical uncertainties. We also show that the polarization of the top quark in W -gluon fusion can be detected at the Fermilab Tevatron and the CERN LHC.

1 Introduction

Single-top-quark production at the Fermilab Tevatron and the CERN Large Hadron Collider (LHC) provides an opportunity to study the charged-current weak-interaction of the top quark [1, 2, 3, 4, 5, 6, 7]. Within the standard model, single-top-quark production offers a means to directly measure the Cabibbo-Kobayashi-Maskawa matrix element V_{tb} . Beyond the standard model, it is sensitive to a non-standard Wtb vertex, and to exotic single-top-quark production processes involving new particles [4, 8, 9, 10, 11, 12, 13, 14, 15]. In order to be a useful probe, the measurement of single-top-quark production must be accompanied by an accurate calculation of the standard-model production cross section and experimental acceptance, as well as an analysis of the associated backgrounds.

It is useful to distinguish between three different types of single-top-quark production, based on the virtuality of the W boson. Fig. 1(a) shows the leading-order Feynman diagram for s -channel single-top-quark production [6, 7]. This process has the theoretical advantage of proceeding via quark-antiquark annihilation, so the partonic flux can be constrained from Drell-Yan data [16]. The next-to-leading-order calculation has been performed for this channel [17], as well as a study of the acceptance and backgrounds [7, 18]. Fig. 1(b) shows a Feynman diagram for t -channel single-top-quark production, often referred to as W -gluon fusion [1, 2, 3, 4, 5].¹ The primary advantage of this channel is statistics. The cross section is almost 3 times larger than that of the s -channel process at the Tevatron ($\sqrt{S} = 2$ TeV), and the cross section at the LHC is 100 times larger than at the Tevatron. The production cross section was recently calculated by us at next-to-leading order [19, 20], and the acceptance and backgrounds have been most completely studied in Ref. [18]. Fig. 1(c) shows a Feynman diagram for Wt production, where an on-shell W is produced [5, 21]. This process proceeds via a gluon- b interaction, which makes the cross section negligible at the Tevatron. However, at the LHC it contributes about 20% of the total single-top-quark cross section. Neither the

¹The s -channel process is sometimes referred to as the W^* process; however, the W boson in the t -channel process is also off-shell.

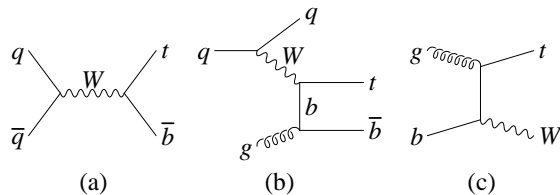


Figure 1: Representative Feynman diagrams for single-top-quark production at hadron colliders: (a) s -channel production, (b) t -channel production (W -gluon fusion), and (c) associated production with a W boson.

next-to-leading-order cross section,² nor the calculation of the acceptance and backgrounds for this process, are yet available.

In this paper we calculate the acceptance and backgrounds for single-top-quark production via W -gluon fusion at the Tevatron and LHC. There are a number of differences with the analysis of Ref. [18]. The most significant improvement is that we perform an accurate calculation of the acceptance, using our next-to-leading-order calculation of the total cross section. This is an essential ingredient in the extraction of the cross section from experiment, and can be used to normalize any future studies. The acceptance cannot simply be calculated by comparing the cross section from Fig. 1(b) with and without cuts, due to the breakdown of perturbation theory in the region where the initial gluon splits into a nearly-collinear $b\bar{b}$ pair. The correct way to treat the collinear region and calculate the acceptance is discussed in detail in Section 2.

Our analysis of backgrounds differs from that of Ref. [18] in that we advocate the use of one and only one b tag to isolate the signal, while Ref. [18] requires one or more b tags. The main motivation for this is that we desire to separate single-top-quark production via W -gluon fusion (which usually has only the b quark from top decay in the fiducial region) from the s -channel process (which usually has a b and a \bar{b} in the fiducial region). This provides two independent measurements of V_{tb} , with different backgrounds and theoretical uncertainties. Perhaps more importantly, the two processes are generally influenced by new

²The next-to-leading-order cross section is available for the identical process of Wc production [22].

physics in different ways, so the deviation of each process from the standard model would be a useful diagnostic [4, 8, 9, 10, 11, 12, 13, 14, 15]. We also perform an analysis of W -gluon fusion at the LHC, while the study of Ref. [18] concentrated on the Tevatron.

Based on these results, we study the sensitivity with which V_{tb} can be extracted from single-top-quark production via W -gluon fusion at both the Tevatron and the LHC, taking into account both statistical and theoretical uncertainties. We also perform an analysis of the s -channel process, and compare the results with those of the W -gluon-fusion process. We consider the data collected during Run I at the Tevatron ($\sqrt{S} = 1.8$ TeV) from 1992–1995 (110 pb⁻¹), the data that will be collected in Run II ($\sqrt{S} = 2$ TeV) beginning in 2000 (2 fb⁻¹), and additional data which may be collected (at the same energy) beyond Run II (30 fb⁻¹).

Since the top quark is produced via the weak interaction in single-top-quark processes, it has significant polarization [4, 5]. An optimal basis for the measurement of this polarization, both for the s -channel process and for W -gluon fusion, was recently introduced in Ref. [23]. We quantify the integrated luminosity required to observe this polarization, including the effects of acceptance and jet resolution.

The paper is organized as follows. In Section 2 we calculate the acceptance for single-top-quark production via W -gluon fusion. We pay particular attention to the issues associated with the splitting of the initial gluon into a nearly-collinear $b\bar{b}$ pair. In Section 3 we briefly discuss our calculational techniques. In Section 4 we present results for the signal and backgrounds at the Tevatron and the LHC, and analyze the accuracy with which V_{tb} can be extracted. Section 5 contains an analysis of the s -channel process. Section 6 is concerned with the polarization of the top quark in single-top-quark processes. We summarize our results in Section 7.

2 Acceptance

We recently calculated the next-to-leading-order total cross section for single-top-quark production via W -gluon fusion in Ref. [20]. The results are listed in Table 1. Experimentally, only the cross section which lies within the geometrical acceptance of the detector is measurable, so it is important to calculate this acceptance. Normally this is straightforward; one simply computes the ratio of the tree-level cross section with and without cuts. However, the total cross section for W -gluon fusion cannot simply be calculated from Fig. 1(b), because perturbation theory breaks down in the region where the initial gluon splits into a nearly-collinear $b\bar{b}$ pair. Thus we must consider the correct way to calculate the acceptance.

The p_T spectrum of the \bar{b} antiquark is shown in Fig. 2. It is peaked at small p_T , because the internal b -quark propagator is close to being on shell when the initial gluon splits into a nearly-collinear $b\bar{b}$ pair. Since $d\sigma/dp_T^2 \sim 1/(p_T^2 + m_b^2)$, the cross section with the p_T of the \bar{b} antiquark above p_{Tcut} is proportional to $\ln[m_t^2/(p_{Tcut}^2 + m_b^2)]$. Another power of this logarithm appears at every order in perturbation theory via collinear gluon radiation from the internal b quark, so the expansion parameter is $\alpha_s \ln[m_t^2/(p_{Tcut}^2 + m_b^2)]$. Thus the calculation of the cross section is more accurate the larger the choice of p_{Tcut} .

Unfortunately, it is not practical to simply choose a large value of p_{Tcut} and measure the cross section for $Wb\bar{b}j$ (j denotes the light-quark jet from the emission of the t -channel W boson in Fig. 1(b); Wb are the decay products of the t quark). There is a large background from $t\bar{t}$ production, which yields the final state $WWb\bar{b}$; this mimics the signal when the additional W boson decays to two jets, and one jet is missed. To suppress this background we search for the signal in the final state Wbj , *i.e.*, we demand that the \bar{b} antiquark *not* appear in the final state.

Fortunately, the cross section with the \bar{b} antiquark below p_{Tcut} can be calculated with good accuracy, provided p_{Tcut} is sufficiently large. This is achieved via a two-step procedure. In Ref. [20] we calculated the total cross section ($p_{Tcut} = 0$) and summed the logarithmically-enhanced terms, $\alpha_s^n \ln^n(m_t^2/m_b^2)/n!$, to all orders [4, 5, 33, 34, 35]. To calculate the cross

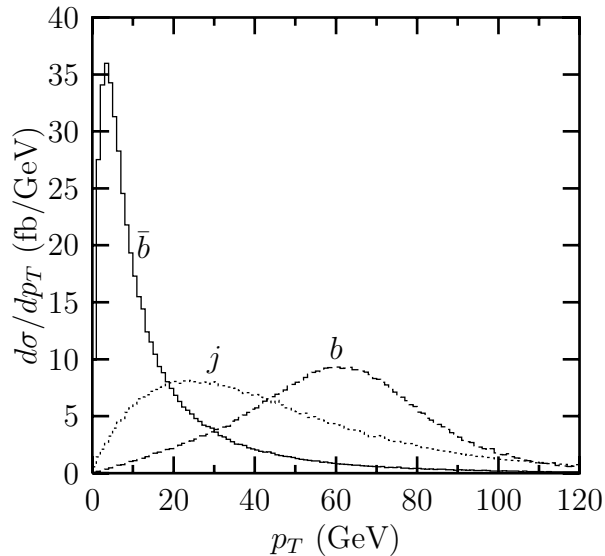


Figure 2: Transverse momentum distributions of the \bar{b} antiquark (solid line), the b quark from top decay (dashed line), and the light-quark jet (dotted line), in single-top-quark production via W -gluon fusion ($gq \rightarrow t\bar{b}q$) at the Tevatron ($\sqrt{S} = 2$ TeV).

section with the \bar{b} antiquark *below* p_{Tcut} , we simply take the total cross section and subtract from it the cross section with the \bar{b} antiquark *above* p_{Tcut} .³

$$\sigma(p_T < p_{Tcut}) = \sigma_{NLO} - \sigma(p_T > p_{Tcut}) . \quad (1)$$

This is tantamount to integrating the transverse momentum of the \bar{b} antiquark over all momenta below p_{Tcut} .

We give in Table 1 the cross section for single-top-quark production via W -gluon fusion with the \bar{b} antiquark below $p_{Tcut} = 20$ GeV. These numbers can be used to normalize future studies. For example, Ref. [18] studied the signal in the final state Wbq , using the process $qb \rightarrow qt$ to approximate the W -gluon-fusion process, and normalizing to the total cross section. However, it is more accurate to normalize to the cross section with the \bar{b} antiquark below some chosen p_{Tcut} (20 GeV in Ref. [18]).⁴ HERWIG and PYTHIA⁵ also simulate

³The cross section with the \bar{b} antiquark above p_{Tcut} is calculated using the scale $\mu^2 = p_T^2 + m_b^2$ in the gluon distribution function and the strong coupling.

⁴Ref. [18] normalized to a cross section of 1.6 pb; we see from Table 1 that a more accurate cross section is 1.90 pb.

⁵PYTHIA uses backwards evolution of the initial-state b distribution function to give the initial $g \rightarrow b\bar{b}$

Table 1: Cross sections (pb) for single-top-quark production via W -gluon fusion with $m_t = 175$ GeV. The next-to-leading-order total cross section is taken from Ref. [20]. The last column gives the cross section with the \bar{b} antiquark below $p_{Tcut} = 20$ GeV. The uncertainty is estimated from the scale variation of the cross section, and does not include the uncertainty in the parton distribution functions nor the uncertainty in the top-quark mass.

\sqrt{S}	σ_{NLO}	$\sigma(p_T < 20 \text{ GeV})$
1.8 TeV $p\bar{p}$	1.70 ± 0.09	1.32 ± 0.14
2 TeV $p\bar{p}$	2.44 ± 0.12	1.86 ± 0.20
14 TeV pp	245 ± 12	164 ± 14

single-top-quark production via W -gluon fusion using $qb \rightarrow qt$.

Our strategy is therefore as follows. We use the process in Fig. 1(b) to calculate the differential cross section for single-top-quark production via W -gluon fusion, using the scale $\mu^2 = p_T^2 + m_b^2$ in the gluon distribution function and the strong coupling.⁶ If the p_T of the \bar{b} antiquark is below p_{Tcut} , we normalize to the cross section calculated as described above. This yields most of the signal cross section (Wbq in the fiducial region). If the p_T of the \bar{b} antiquark is *above* p_{Tcut} , we simply use the cross section obtained from Fig. 1(b). This yields the final state $Wb\bar{b}q$, which we reject if all three jets are in the fiducial region, but which contributes to the signal if one jet is missed, one and only one of the two remaining jets is b -tagged and it, together with the W boson, reconstructs to the top-quark mass (within some resolution). This strategy avoids the occurrence of powers of $\alpha_s \ln(m_t^2/m_b^2)$ at higher orders in perturbation theory, which would degrade the accuracy of the calculation.

2.1 Theoretical uncertainty

In Ref. [20], we studied the uncertainty in the next-to-leading-order total cross section for single-top-quark production via W -gluon fusion by varying the scale in the b -quark distribution function and the strong coupling. This indicated an uncertainty in the total cross

splitting.

⁶We use the scale $\mu^2 = Q^2$, where Q^2 is the virtuality of the t -channel W boson, for the light-quark distribution function [20].

section of $\pm 5\%$, not including the uncertainty in the parton distribution functions and the top-quark mass. However, to obtain the cross section with the p_T of the \bar{b} antiquark below p_{Tcut} , we need to subtract from the total cross section the cross section with the p_T of the \bar{b} antiquark above p_{Tcut} , as discussed above. Since the latter is a tree-level calculation, its scale dependence is relatively large. We use the scale $\mu^2 = p_T^2 + m_b^2$ in the gluon distribution function and the strong coupling, and find a $\pm 30\%$ uncertainty in this cross section at the Tevatron ($\pm 15\%$ at the LHC) by varying μ between one half and twice this value. We add in quadrature the absolute uncertainty in the total cross section and the cross section with the p_T of the \bar{b} antiquark above p_{Tcut} . This yields a relative uncertainty in the cross section with the p_T of the \bar{b} antiquark below p_{Tcut} of about $\pm 10\%$ at both the Tevatron and the LHC.⁷ This is reflected in the uncertainty in the numbers in the last column of Table 1. To reduce this uncertainty would require the resummation of the large logarithms $\alpha_s^n \ln^n [m_t^2 / (p_{Tcut}^2 + m_b^2)] / n!$ which appear in the calculation of the cross section with the p_T of the \bar{b} antiquark above p_{Tcut} .

Another source of uncertainty in the cross section is the uncertainty in the parton distribution functions, especially the gluon distribution function. This uncertainty has recently been studied in Ref. [24], and it appears to be less than $\pm 10\%$ at both the Tevatron and the LHC. This is comparable to the uncertainty stemming from the scale variation described above. That study indicates that the uncertainty in the parton distribution functions could potentially be pushed below $\pm 10\%$.

The uncertainty in the top-quark mass also leads to an uncertainty in the cross section [20]. The present uncertainty in the top-quark mass of ± 5.2 GeV [25] corresponds to an uncertainty in the cross section of $\pm 9\%$ at the Tevatron. Anticipating an uncertainty of ± 3 GeV from Run II at the Tevatron [18] corresponds to an uncertainty in the cross section of $\pm 5\%$, much less than the uncertainty from the scale variation and the parton distribution

⁷Although the uncertainty in the cross section with the p_T of the \bar{b} antiquark above p_{Tcut} is half as large at the LHC compared with the Tevatron, the cross section itself is a larger fraction of the total cross section at the LHC (see Table 1). This is why the uncertainty in the cross section with the p_T of the \bar{b} antiquark below p_{Tcut} is comparable at the Tevatron and the LHC.

functions. The uncertainty in the top-quark mass at the Tevatron and the LHC will ultimately reach ± 2 GeV or less [18], corresponding to an uncertainty in the cross section of $\pm 3\%$ at the Tevatron, and $\pm 2\%$ at the LHC.

Combining all theoretical uncertainties in quadrature, we estimate a theoretical uncertainty of about $\pm 15\%$ in the cross section at the Tevatron and the LHC, assuming an uncertainty in m_t of ± 3 GeV or less.

3 Calculation

The top-quark mass is taken to be 175 GeV [25]. We optimize our study for the dominant single-top-quark production mechanism, W -gluon fusion. The final state, $Wb\bar{b}j$, consists of a recoiling light-quark jet from the production of the t -channel W boson, a \bar{b} antiquark from the splitting of the initial gluon, and the decay products of the top quark. As discussed in the previous section, the large $t\bar{t}$ background requires that we use Wbj as our signal, *i.e.*, we reject events in which the \bar{b} antiquark is detected above some p_{Tcut} . Thus our signal is a leptonically-decaying W boson (to reduce QCD backgrounds) plus two jets, with one and only one b tag. In addition to the $t\bar{t}$ background, the other principal backgrounds are $Wb\bar{b}$ and Wjj (with one jet mistagged), as well as $Wc\bar{c}$ and Wcj (with one c quark mistagged). The background WZ , with $Z \rightarrow b\bar{b}$, is small and can be neglected.⁸ Requiring one and only one b tag helps reduce the $t\bar{t} \rightarrow WWb\bar{b}$, $Wb\bar{b}$, and $Wc\bar{c}$ backgrounds, while maintaining almost all of the signal.

The signal and backgrounds for single-top-quark production are calculated using tree-level matrix elements generated by MadGraph [27]. The normalization of the W -gluon-fusion cross section is determined as described in Section 2. The s -channel process is normalized to the next-to-leading-order cross section [17]. The $t\bar{t}$ cross section is normalized to the next-to-leading-order result [28, 29],⁹ not including soft-gluon resummation [30, 31, 32]. The $Wb\bar{b}$, $Wc\bar{c}$, Wcj , and Wjj cross sections are calculated at leading order using the CTEQ4L [36]

⁸In contrast, WZ with $Z \rightarrow b\bar{b}$ is an important background to WH with $H \rightarrow b\bar{b}$, because M_Z is near m_H in the Higgs mass range of interest [26].

⁹We use the central values given in the last paper of Ref. [30].

parton distribution functions with the renormalization and factorization scales chosen to be $\mu^2 = \hat{s}$. Since these cross sections will be measured in the invariant-mass regions away from the top-quark mass, theoretical uncertainties in the normalization of these backgrounds will not limit the accuracy of the measurement of the signal cross section. The $gb \rightarrow Wt$ cross section is also calculated at leading order using CTEQ4L and $\mu^2 = \hat{s}$.

We smear the jet energies with a Gaussian function of width $\Delta E_j/E_j = 0.80/\sqrt{E_j} \oplus 0.05$ (added in quadrature) to simulate the resolution of the hadron calorimeter. The momenta of overlapping jets ($\Delta R_{jj} < 0.7$) are added and the resulting momentum is associated with a single jet. We do not smear the lepton energy, since this is a small effect compared with the smearing of the jet energies. The lepton must be separated from the jets ($\Delta R_{j\ell} > 0.7$) or it is considered missed. The two solutions for the neutrino momentum which satisfy the missing- p_T and W -mass constraints are reconstructed and the solution with the smallest magnitude of rapidity is chosen. This reconstructed event must pass the cuts listed in Table 2 used to simulate the acceptance of the detector. The rapidity and p_T coverage are chosen to simulate a generic detector. Most of the jets are central at the Tevatron, so it is only necessary to have jet coverage to $|\eta_j| < 2.5$, while the jets are distributed over a wider range of rapidities at the LHC, necessitating coverage to $|\eta_j| < 4$. Experimental results will be modified depending on actual detector capabilities.

We assume a b -tagging efficiency of 60% (50% for Run I) with a mistag rate of 15% for charm quarks and 0.5% for light quarks at both the Tevatron [18, 37] and the LHC [38]. As we shall see, the large charm background suggests it may be advantageous to employ a strategy to reject charm (and light-quark) jets. We quantify the usefulness of increased charm and light-quark rejection in the search for single-top-quark production in the Tevatron Run I data.

The p_T spectrum of the \bar{b} antiquark, the b quark from the top decay, and the light-quark jet from the emission of the t -channel W boson, from single-top-quark production via W -gluon fusion, are shown in Fig. 2. The b -quark p_T spectrum peaks at about 60 GeV, and the light-quark jet has a broad p_T spectrum, while the \bar{b} antiquark is produced mostly at low

Table 2: Cuts used to simulate the acceptance of the detector. The rapidity coverage for jets is taken to be $|\eta_j| < 2.5$ at the Tevatron and $|\eta_j| < 4$ at the LHC. The rapidity coverage for b tagging is taken to be $|\eta_b| < 1$ at Tevatron Run I, and $|\eta_b| < 2$ at Tevatron Run II and beyond, as well as at the LHC. The $p_{T\ell}$ threshold is greater for charged leptons which are used as triggers (in parentheses).

$$\begin{array}{ll}
|\eta_b| < 2 & (1) \quad p_{Tb} > 20 \text{ GeV} \\
|\eta_\ell| < 2.5 & p_{T\ell} > 10 \text{ GeV} \text{ (20 GeV)} \\
|\eta_j| < 2.5 & (4) \quad p_{Tj} > 20 \text{ GeV} \\
|\Delta R_{jj}| > 0.7 & |\Delta R_{j\ell}| > 0.7 \\
\not{p}_T > 20 \text{ GeV} &
\end{array}$$

p_T . Hence the majority of our signal comes from tagging the b quark, with the light quark providing the second jet.¹⁰ However, we include in our signal *any* final state with two and only two jets with $p_T > 20$ GeV, with one and only one b tag.

4 Results

Our results are summarized in Table 3. The first column shows the total cross section times the branching ratio (2/9) for the top quark to decay semileptonically (not including the τ lepton, which is treated as a jet). The signal cross section includes both t and \bar{t} production. Similarly, the $Wb\bar{b}$, $Wc\bar{c}$, Wcj , and Wjj backgrounds account for both W^+ and W^- production times the branching ratio 2/9. The $t\bar{t}$ background is multiplied by the branching ratio 4/9 to include the possibility that either the t or the \bar{t} decays semileptonically (a $t\bar{t}$ event can be a background to either single t or single \bar{t} production).

The second column in Table 3 shows the cross section for events which pass the detector acceptance. These events have one and only one b -tagged jet, and at least one other jet. The numbers in parentheses are the cross sections for events which have a reconstructed $b\ell\nu$ invariant mass within ± 20 GeV of the top-quark mass (to account for jet resolution). About 70% of the single-top-quark events from W -gluon fusion survive this cut at the Tevatron (60% at the LHC), while only about 40% of the $t\bar{t}$ events survive, and only 20% of the

¹⁰After all cuts, this accounts for about 94% of the signal at both the Tevatron and the LHC.

$Wb\bar{b}$, $Wc\bar{c}$, Wcj , and Wjj events survive (at both machines). The low acceptance for these last four backgrounds is easily understood since there is no kinematic preference towards the top-quark mass. The $t\bar{t}$ acceptance is only about 40% because one half of the time the tagged b quark is associated with the other top-quark in the event.

It is evident from Table 3 that the largest background is $t\bar{t} \rightarrow W^+W^-b\bar{b}$, and it is much larger than the signal. This background is particularly worrisome because it produces a peak in the $b\ell\nu$ invariant-mass spectrum at the top-quark mass, just as does the signal.¹¹ Hence it is important to apply additional cuts to reduce this background. Since this background has an additional W boson in the final state, we reject events which have an additional charged lepton¹² with $p_{T\ell} > 10$ GeV, or an additional jet with $p_{Tj} > 20$ GeV and $|\eta_j| < 2.5$ at the Tevatron¹³ ($|\eta_j| < 4$ at the LHC). This reduces the $t\bar{t}$ background by a factor of 15 in the peak region at both the Tevatron and the LHC, while reducing the signal by only a modest amount, since the signal rarely has a third jet with $p_{Tj} > 20$ GeV. This “veto” [39] yields the signal and background cross sections listed in the third column of Table 3.

We show the $b\ell\nu$ invariant-mass distribution for single-top-quark production and the various backgrounds at the Tevatron ($\sqrt{S} = 2$ TeV) in Fig. 3, and at the LHC in Fig. 4. The W -gluon-fusion process is prominent at both the Tevatron and the LHC,¹⁴ but the backgrounds are non-negligible. The $t\bar{t}$ background has been reduced to an acceptable level, but it is still significant, and because it has the same shape as the signal it will be necessary to know the normalization of this background independently. This could be achieved by measuring the $t\bar{t}$ cross section using the full $W^+W^-b\bar{b}$ final state, and then calculating its contribution to the Wbj background, as we have done. Since we desire to separate single-top-quark production via W -gluon fusion from the s -channel process, it will also be necessary to measure the latter and subtract it from the signal. This can be achieved by double b tagging

¹¹In contrast, the $t\bar{t}$ background is not as problematic for the process WH with $H \rightarrow b\bar{b}$, because it does not produce a peak in the $b\bar{b}$ invariant mass near the Higgs mass [26].

¹²The τ lepton is treated as a jet.

¹³Increasing the jet rapidity coverage to $|\eta_j| < 4$ at the Tevatron does not decrease this background significantly.

¹⁴One of the factors contributing to the prominence of the signal, in comparison with the study in Ref. [18], is that a poorer jet energy resolution was assumed in that study.

Table 3: Cross sections (fb) for single-top-quark production and a variety of background processes at the Tevatron and the LHC. The W -gluon-fusion signal is denoted by $t\bar{b}j$, and the s -channel process by $t\bar{b}$. The first column is the total cross section for $t + \bar{t}$ production times the branching ratio (2/9) of the W boson to e, μ . The $t\bar{t}$ background is multiplied by a branching ratio of 4/9 to account for either the t or the \bar{t} decaying semileptonically. The second column adds the cuts listed in Table 2 to simulate the acceptance of the detector, and also includes a b -tagging efficiency of 60% (50% for Run I) with a mistag rate of 15% for charm and 0.5% for light-quark jets. Listed in parentheses is the cross section for events in which the reconstructed $b\ell\nu$ invariant mass is within ± 20 GeV of the top-quark mass. The third column includes a jet veto $p_T < 20$ GeV to reduce the $t\bar{t}$ background.

	Tevatron Total \times BR	1.8 TeV $p\bar{p}$ Detector (peak)	Veto (peak)
$t\bar{b}j$	378	61 (41)	46 (33)
$t\bar{b}$	162	36 (18)	36 (18)
Wt	16	6.1 (3.1)	1.4 (0.8)
$Wb\bar{b}$	6500	106 (20)	106 (20)
$Wc\bar{c}$	—	44 (8)	44 (8)
Wcj	—	136 (24)	136 (24)
Wjj	—	127 (25)	127 (25)
$t\bar{t}$	2160	551 (240)	47 (13)

	Tevatron Total \times BR	2 TeV $p\bar{p}$ Detector (peak)	Veto (peak)
$t\bar{b}j$	542	133 (90)	107 (76)
$t\bar{b}$	196	48 (24)	48 (24)
Wt	26	16 (8.4)	3.8 (2.1)
$Wb\bar{b}$	7420	146 (28)	146 (28)
$Wc\bar{c}$	—	74 (14)	74 (14)
Wcj	—	274 (53)	274 (53)
Wjj	—	257 (54)	257 (54)
$t\bar{t}$	2980	838 (364)	80 (24)

	LHC Total \times BR	14 TeV pp Detector (peak)	Veto (peak)
$t\bar{b}j$	54400	12500 (7510)	8930 (6110)
$t\bar{b}$	2270	470 (229)	470 (229)
Wt	13700	7510 (3610)	1650 (820)
$Wb\bar{b}$	70700	1140 (230)	1140 (230)
$Wc\bar{c}$	—	750 (150)	750 (150)
Wcj	—	24200 (5070)	24200 (5070)
Wjj	—	7000 (1460)	7000 (1460)
$t\bar{t}$	357000	95600 (40700)	9040 (2770)

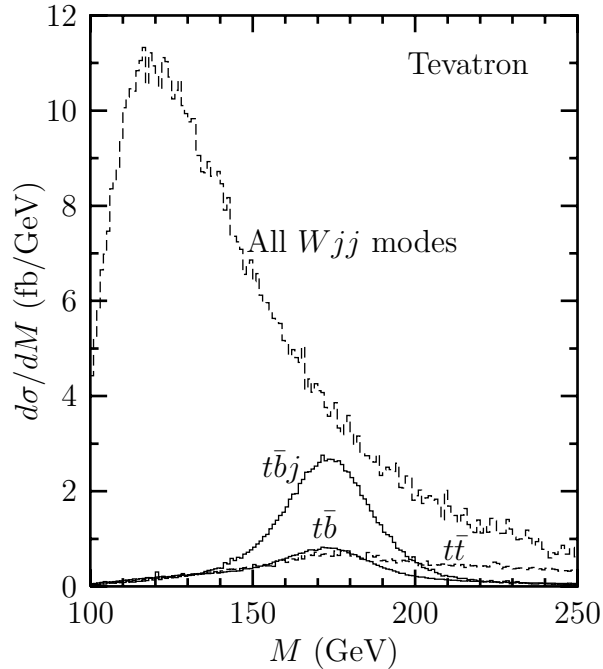


Figure 3: The $bl\nu$ invariant-mass (M) distribution for single-top-quark production and backgrounds at the Tevatron ($\sqrt{S} = 2$ TeV) with single b tagging. The W -gluon-fusion signal is denoted by $t\bar{b}j$, and the s -channel process by $t\bar{b}$ (the Wt process is negligibly small). The Wjj background includes $Wb\bar{b}$, $Wc\bar{c}$, Wcj , and Wjj . The $t\bar{t}$ background is shown separately.

[7], as discussed in Section 5. This is unnecessary at the LHC, where the s -channel process is negligible.

The remaining backgrounds — $Wb\bar{b}$, $Wc\bar{c}$, Wcj , and Wjj — all yield continuous spectra, and can therefore be calibrated by measuring them in the invariant-mass regions away from the peak region. These backgrounds are significant and comparable to each other at the Tevatron, but only Wcj is significant at the LHC. It may be desirable to reject more strongly events in which a charm or light quark fakes a b jet, at both the Tevatron and the LHC. The VXD3 vertex detector in SLD has achieved a b -tagging efficiency of 50%, with a mistag rate of only 1.24% from charm and 0.07% from light quarks [40, 41].

The statistics for discovering a signal are different from those for measuring its cross section. To claim a discovery, one needs to demonstrate that the signal is not consistent

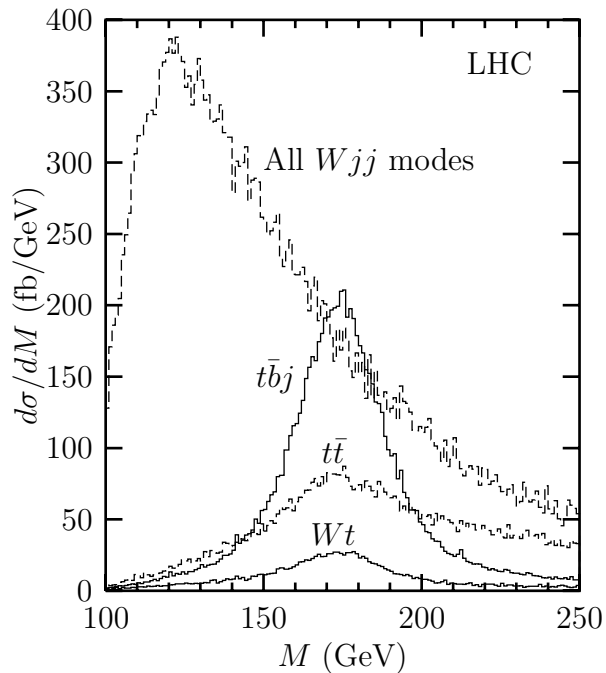


Figure 4: The $b\ell\nu$ invariant-mass (M) distribution for single-top-quark production and backgrounds at the LHC with single b tagging. The W -gluon-fusion signal is denoted by $t\bar{b}j$, and the Wt process is also shown (the s -channel process is negligibly small). The Wjj background includes $Wb\bar{b}$, $Wc\bar{c}$, Wcj , and Wjj . The $t\bar{t}$ background is shown separately.

Table 4: Statistical significance of the signal (S/\sqrt{B}) and accuracy of the measured cross section ($\sqrt{S+B}/S$) for single-top-quark production via W -gluon fusion at the Tevatron and the LHC. Also given is the accuracy of the extracted value of V_{tb} , assuming a $\pm 15\%$ uncertainty in the theoretical cross section.

	S/\sqrt{B}	$\sqrt{S+B}/S$	$\Delta V_{tb}/V_{tb}$
1.8 TeV $p\bar{p}$ (110 pb $^{-1}$)	1.8	69%	35%
2 TeV $p\bar{p}$ (2 fb $^{-1}$)	11	12%	10%
2 TeV $p\bar{p}$ (30 fb $^{-1}$)	43	3.0%	7.6%
14 TeV pp (1 fb $^{-1}$)	73	1.8%	7.6%

with a fluctuation in the background. The discovery significance is therefore governed by the number of signal events divided by the square root of the number of background events, S/\sqrt{B} . On the other hand, the accuracy with which a cross section can be measured is limited by the fluctuation in the total number of expected events in the signal region, $S+B$. Thus the fractional uncertainty in the measured cross section is $\sqrt{S+B}/S$.

We list in Table 4 the statistical significance of the single-top-quark signal, and the statistical uncertainty in the measured cross section, at the Tevatron and the LHC. All three single-top-quark production processes have been regarded as part of the signal in determining these numbers, although W -gluon fusion is dominant.¹⁵ We see that there is not sufficient data to discover single-top-quark production in the Tevatron Run I data, and the cross section can be measured only crudely. As mentioned above, it may be possible to increase the rejection of charm and light-quark jets. However, even if it were possible to achieve 100% rejection while maintaining the 50% b -tagging efficiency the significance of the signal would be only 3σ , not enough for discovery, but perhaps enough for “evidence” of single-top-quark production in Run I.

Single-top-quark production should be discovered (5σ) at Run II with about 500 pb $^{-1}$ of integrated luminosity, and the cross section will ultimately be measured to an accuracy of

¹⁵The significance and statistical sensitivity for single-top-quark production via W -gluon fusion alone are somewhat less, because the s -channel process and the Wt process must then be considered as backgrounds.

$\pm 12\%$ with 2 fb^{-1} of integrated luminosity. This is comparable to the theoretical accuracy, which we estimated to be $\pm 15\%$ in Section 2.1. Combined in quadrature, and neglecting any systematic uncertainties, we conclude that V_{tb} can be measured to an accuracy of $\pm 10\%$ in Run II at the Tevatron (assuming $V_{tb} \approx 1$).

Additional running at the Tevatron will reduce the statistical uncertainty further. An integrated luminosity of 30 fb^{-1} yields a statistical uncertainty in the cross section of only $\pm 3\%$. Together with the $\pm 15\%$ theoretical uncertainty, this yields an uncertainty in V_{tb} of $\pm 7.6\%$. In order to maximally benefit from the reduced statistical uncertainty, it is necessary to reduce the theoretical and systematic uncertainties to a level comparable to the statistical uncertainty. The study of Ref. [24] suggests that the uncertainty in the quark-gluon luminosity can be reduced below $\pm 10\%$. The scale uncertainty in the cross section of $\pm 10\%$ requires additional theoretical work to reduce, as discussed in Section 2.1. We have not attempted to estimate the experimental systematic uncertainties.

The statistical uncertainty at the LHC is only 1.8% with just 1 fb^{-1} of integrated luminosity. The accuracy with which V_{tb} can be measured will therefore be limited entirely by the theoretical and systematic uncertainties. It is a challenge to reduce these to a level such that one can benefit from the tremendous statistical sensitivity of the LHC.

4.1 Forward jet tag

The emission of the virtual t -channel W boson in single-top-quark production via W -gluon fusion [Fig. 1(b)] results in a high-rapidity jet in the final state [2, 3, 5]. The same phenomenon occurs for Higgs production via WW fusion, and the tagging of this forward jet has been advocated to isolate the signal from the background for a heavy Higgs boson [39, 42, 43, 44]. In this section we investigate whether this feature of W -gluon fusion can be used to increase the statistical significance (S/\sqrt{B}) of our signal.

We perform the same analysis as above, but we demand that the non- b -tagged jet have a rapidity whose magnitude is greater than η_{cut} . Before imposing the jet veto, we find that the significance rises slightly as η_{cut} is increased from zero, and then eventually decreases.

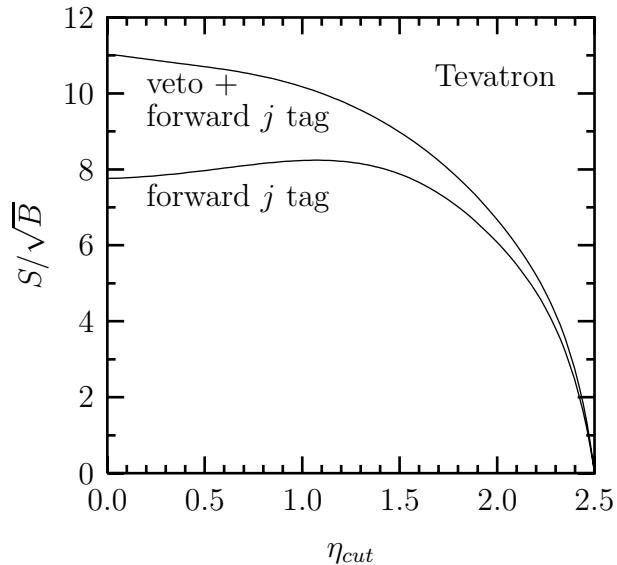


Figure 5: Significance of the single-top-quark signal in Run II at the Tevatron ($\sqrt{S} = 2$ TeV, 2 fb^{-1}) versus the minimum rapidity of the non- b -tagged jet in the signal. Curves are shown with and without the jet veto imposed.

This is shown in Fig. 5 at the Tevatron ($\sqrt{S} = 2$ TeV), and the result is similar at the LHC. However, after imposing the jet veto, we find that the significance decreases as η_{cut} is increased from zero, and is always greater than the significance without the veto. This is also shown in Fig. 5. Thus this simple forward jet tag does not increase the significance of the signal. However, this forward jet is a characteristic of single-top-quark production via W -gluon fusion, and its observation would build confidence that one has observed this process.

5 Comparison with s -channel single-top-quark production

The s -channel production of single top quarks, shown in Fig. 1(a), also provides a means to measure the CKM matrix element V_{tb} [6, 7]. Furthermore, the s -channel and t -channel (W -gluon fusion) processes generally have different dependence on new physics, so it is worthwhile to measure them separately [4, 8, 9, 10, 11, 12, 13, 14, 15]. In this section we

calculate the sensitivity of the Tevatron to V_{tb} via the s -channel process, and compare it with the results for W -gluon fusion presented in the previous section.

The final state in s -channel production of single top quarks is $Wb\bar{b}$. It can be separated from single-top-quark production via W -gluon fusion by double b tagging, since W -gluon fusion usually produces only one b jet with $p_T > 20$ GeV. The s -channel process has a smaller cross section than W -gluon fusion, and the efficiency of double b -tagging is less than that of single b tagging, so the statistical sensitivity is less for the s -channel process. However, this is compensated by the smaller theoretical uncertainty in the cross section [7, 17].

The analysis of signal and backgrounds follows closely that of W -gluon fusion. However, because we now demand two b tags, the backgrounds are generally smaller, with the exception of $Wb\bar{b}$ and $t\bar{t} \rightarrow WWb\bar{b}$, which also contain two b jets in the final state. To select the correct b jet to associate with the top quark, we use the fact that in $q\bar{q} \rightarrow t\bar{b}$ the b quark from top decay tends to go in the proton direction in $p\bar{p}$ collisions [6, 7]. As in the W -gluon-fusion analysis, we choose the solution for the neutrino momentum which has the smallest magnitude of rapidity.¹⁶

The results are presented in Table 5. As in the W -gluon fusion analysis, a jet veto is necessary to suppress the enormous $t\bar{t}$ background. The resulting $bl\nu$ invariant-mass distribution is shown in Fig. 6 at the Tevatron ($\sqrt{S} = 2$ TeV) and in Fig. 7 at the LHC. The signal is prominent at the Tevatron, although the backgrounds are non-negligible. The situation is less promising at the LHC, due to the large $t\bar{t}$ background, which has the same shape as the signal. Furthermore, the majority of signal events come from W -gluon fusion, not from the s -channel process, so the double- b -tag strategy does not succeed in isolating the s -channel process at the LHC. We henceforth concentrate our analysis on the Tevatron results.

We list in Table 6 the discovery significance (S/\sqrt{B}) and the statistical accuracy ($\sqrt{S+B}/S$) for s -channel production of single top quarks. As with W -gluon fusion, there is not enough

¹⁶Our analysis is essentially the same as Ref. [7], with the exception that we do not make the cut $M(b\bar{b}) > 110$ GeV, which was made to suppress the $WZ \rightarrow Wb\bar{b}$ background. We have found this cut to be unnecessary, as this background is modest in the signal region, $M(bl\nu) \approx m_t$, as evidenced by the results in Table 5.

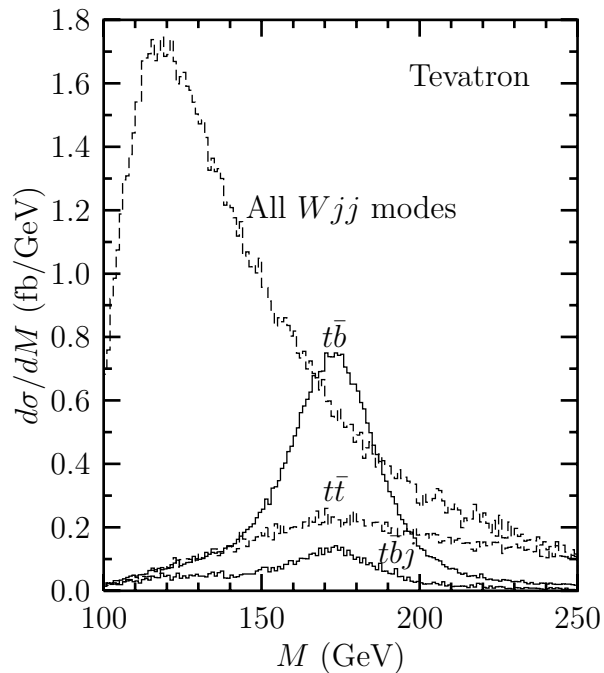


Figure 6: The $bl\nu$ invariant-mass (M) distribution for single-top-quark production and backgrounds at the Tevatron ($\sqrt{S} = 2$ TeV) with double b tagging. The s -channel signal is denoted by $t\bar{b}$, and the W -gluon-fusion process by $t\bar{b}j$ (the Wt process is negligibly small). The Wjj background is dominated by $Wb\bar{b}$. The $t\bar{t}$ background is shown separately.

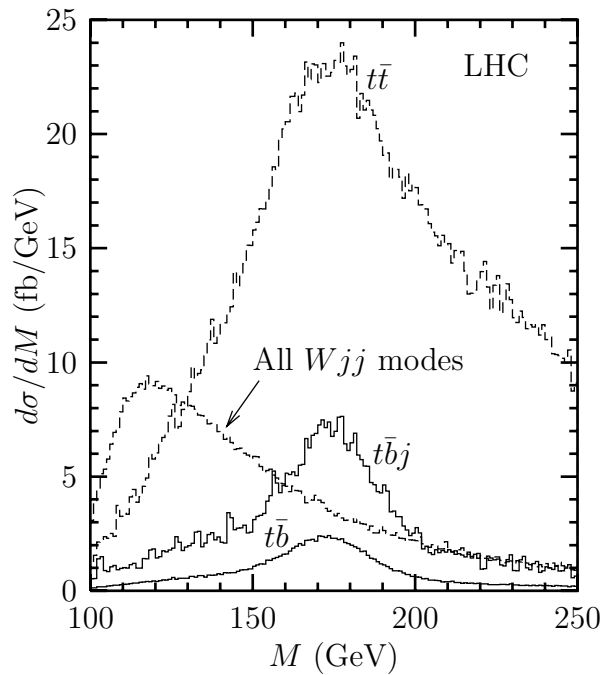


Figure 7: The $bl\nu$ invariant-mass (M) distribution for single-top-quark production and backgrounds at the LHC with double b tagging. The s -channel signal is denoted by $t\bar{b}$, and the W -gluon-fusion process by $t\bar{b}j$ (the Wt process is negligibly small). The Wjj background is dominated by $Wb\bar{b}$. The $t\bar{t}$ background is shown separately.

Table 5: Cross sections (fb) for single-top-quark production and a variety of background processes at the Tevatron and the LHC. The s -channel signal is denoted by $t\bar{b}$, and the W -gluon-fusion process is denoted by $t\bar{b}j$. The analysis is as described in the caption of Table 3, except we have required two b tags instead of one and only one b tag.

	Tevatron Total \times BR	1.8 TeV $p\bar{p}$ Detector (peak)	Veto (peak)
$t\bar{b}$	162	8.9 (5.5)	8.9 (5.5)
$t\bar{b}j$	378	4.4 (2.3)	1.5 (0.7)
Wt	16	0.04 (0.01)	0.03 (0.01)
$Wb\bar{b}$	6500	29 (5.1)	29 (5.1)
WZ	58	2.5 (0.6)	2.5 (0.6)
$Wc\bar{c}$	—	2.6 (0.5)	2.6 (0.5)
Wcj	—	0.35 (0.06)	0.35 (0.06)
Wjj	—	0.28 (0.05)	0.28 (0.05)
$t\bar{t}$	2160	136 (61)	8.4 (2.6)

	Tevatron Total \times BR	2 TeV $p\bar{p}$ Detector (peak)	Veto (peak)
$t\bar{b}$	196	32 (21)	32 (21)
$t\bar{b}j$	542	21 (11)	7 (4)
Wt	26	0.1 (0.04)	0.1 (0.04)
$Wb\bar{b}$	7420	97 (18)	97 (18)
WZ	71	10 (2.2)	10 (2.2)
$Wc\bar{c}$	—	6.3 (1.2)	6.3 (1.2)
Wcj	—	1.2 (0.2)	1.2 (0.2)
Wjj	—	0.6 (0.1)	0.6 (0.1)
$t\bar{t}$	2980	496 (223)	28 (8)

	LHC Total \times BR	14 TeV pp Detector (peak)	Veto (peak)
$t\bar{b}$	2270	209 (103)	209 (103)
$t\bar{b}j$	54400	2055 (932)	492 (221)
Wt	13700	44 (15)	41 (14)
$Wb\bar{b}$	70700	544 (112)	544 (112)
WZ	880	50 (14)	50 (14)
$Wc\bar{c}$	—	51 (10)	51 (10)
Wcj	—	83 (17)	83 (17)
Wjj	—	13 (3)	13 (3)
$t\bar{t}$	357000	44800 (19500)	2780 (838)

Table 6: Statistical significance of the signal (S/\sqrt{B}) and accuracy of the measured cross section ($\sqrt{S+B}/S$) for single-top-quark production via the s -channel process at the Tevatron. Also given is the accuracy of the extracted value of V_{tb} , assuming a $\pm 6\%$ uncertainty in the theoretical cross section. We include an uncertainty in the theoretical cross section, due to the uncertainty in the top-quark mass, of $\pm 15\%$ at Run I, $\pm 7.5\%$ at Run II, and $\pm 5\%$ beyond Run II at the Tevatron.

	S/\sqrt{B}	$\sqrt{S+B}/S$	$\Delta V_{tb}/V_{tb}$
1.8 TeV $p\bar{p}$ (110 pb $^{-1}$)	0.7	190%	95%
2 TeV $p\bar{p}$ (2 fb $^{-1}$)	6.5	21%	12%
2 TeV $p\bar{p}$ (30 fb $^{-1}$)	25	5.4%	4.7%

data in Run I for discovery.

Discovery (5σ) will occur in Run II after approximately 1 fb $^{-1}$ of integrated luminosity has been collected, and the cross section will ultimately be measured to $\pm 21\%$ with 2 fb $^{-1}$ of data. The theoretical uncertainty in the cross section is estimated to be about $\pm 6\%$ [17], plus an additional uncertainty from the uncertainty in the top-quark mass. Assuming the mass is measured to ± 3 GeV in Run II [18], this adds an uncertainty in the cross section of $\pm 7.5\%$ [17]. Combining all three uncertainties in quadrature, one finds that V_{tb} will be measured to $\pm 12\%$ via the s -channel process in Run II. This is comparable to the accuracy achieved via W -gluon fusion, which has a smaller statistical uncertainty but a larger theoretical uncertainty.

The small theoretical uncertainty in the s -channel process becomes increasingly relevant with greater integrated luminosity. With 30 fb $^{-1}$ of integrated luminosity, the statistical uncertainty is comparable to the theoretical uncertainty of $\pm 6\%$.¹⁷ Assuming the top-quark mass can be measured to ± 2 GeV with this amount of data [18], there is an additional $\pm 5\%$ uncertainty in the theoretical cross section from the uncertainty in the top-quark mass. Combining all three uncertainties in quadrature, one finds that V_{tb} can be measured to $\pm 4.7\%$ with 30 fb $^{-1}$ of integrated luminosity at the Tevatron. This is better than the $\pm 7.6\%$

¹⁷It is likely that the theoretical uncertainty can be reduced below $\pm 6\%$ with additional work [17].

uncertainty achieved via W -gluon fusion, due to its larger theoretical uncertainty.

6 Polarization

Single-top-quark production proceeds via the weak interaction, so the top quarks produced are highly polarized [4, 5]. The optimal basis for the study of this polarization was recently constructed in Ref. [23]. The top quark is 100% polarized, in the top-quark rest frame, along the direction of the d quark (or \bar{d} antiquark) in the event. Since W -gluon fusion proceeds via $ug \rightarrow dt\bar{b}$ about 77% of the time at the Tevatron ($\sqrt{S} = 2$ TeV), the d quark is usually the light-quark jet. The other 23% of the events proceed via $\bar{d}g \rightarrow \bar{u}t\bar{b}$, in which case the \bar{d} quark is moving along one of the beam directions. However, since the light-(anti)quark (\bar{u}) jet tends to move in the same direction as the \bar{d} antiquark, the direction of the light-quark jet is still a rather good basis to analyze the spin in these events. It is shown in Ref. [23] that the top quark has a net 96% polarization along the direction of the light-quark jet in single-top-quark production via W -gluon fusion at the Tevatron ($\sqrt{S} = 2$ TeV).

Since the top quark decays well before QCD interactions can flip its spin, the polarization of the top quark is observable in the distribution of its decay products [45]. The most sensitive spin analyzer is the charged lepton in semileptonic decay, whose partial width (Γ) has the angular distribution

$$\frac{1}{\Gamma} \frac{d\Gamma}{d\cos\theta} = \frac{1}{2}(1 + \cos\theta) \quad (2)$$

where θ is the angle, in the top-quark rest frame, between the direction of the charged lepton and the spin of the top quark [46]. Thus, in W -gluon-fusion events, the charged lepton from top-quark decay has an angular distribution with respect to the light-quark jet, in the top-quark rest frame, given approximately by Eq. (2).

We show in Fig. 8 the angular distribution of the charged lepton with respect to the direction of the non- b -tagged jet, in the top-quark rest frame, from single-top-quark events at the Tevatron ($\sqrt{S} = 2$ TeV). The expected angular distribution, Eq. (2), is approximately observed, but is degraded by the cuts in Table 2, jet resolution, jet veto, and reconstruction

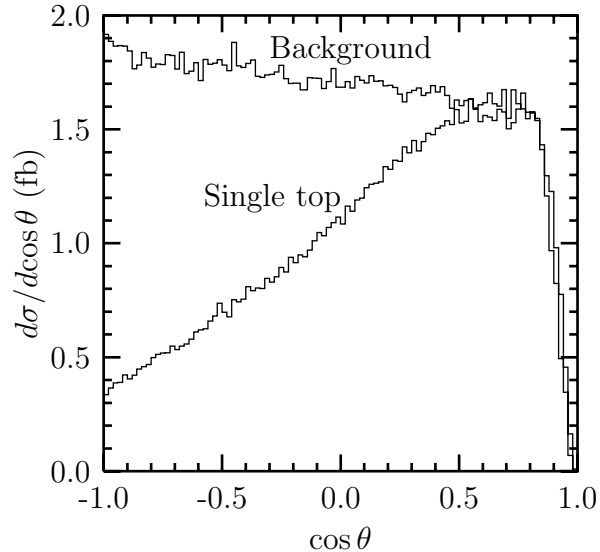


Figure 8: Angular distribution of the charged lepton in single-top-quark events at the Tevatron ($\sqrt{S} = 2$ TeV), with respect to the non- b -tagged jet, in the top-quark rest frame. Also shown is the angular distribution of the sum of all background events. The distributions correspond to the events in the last column of Table 3.

of the neutrino’s momentum, as well as the contribution from the s -channel process. The suppression at $\cos\theta \approx 1$ is due to the $\Delta R_{jl} > 0.7$ cut between the charged lepton and the jet. The other curve is due to the sum of all the backgrounds, and is nearly isotropic (except for the suppression at $\cos\theta \approx 1$), despite the cuts imposed on the events.

A simple test to observe the top-quark polarization in W -gluon fusion is to measure the asymmetry in the angular distribution of the charged lepton, Fig. 8. Since the $\Delta R_{jl} > 0.7$ cut removes the small-angle region, we define an asymmetry between $-1 < \cos\theta < 0.8$:

$$A \equiv \frac{\sigma(-1 < \cos\theta < -0.1) - \sigma(-0.1 < \cos\theta < 0.8)}{\sigma(-1 < \cos\theta < -0.1) + \sigma(-0.1 < \cos\theta < 0.8)} \quad (3)$$

The signal in Fig. 8 has an asymmetry of -38% . An unpolarized top quark would have zero asymmetry, so a nonzero asymmetry measurement would constitute observation of the polarization of the top-quark in W -gluon fusion events. Including the background, the expected asymmetry measurement at the Tevatron is about -14% . Evidence for nonzero asymmetry (3σ) will be available in the Run II data. Observation at the 5σ level takes

approximately 500 signal events, which requires about 5 fb^{-1} of integrated luminosity. The asymmetry is also evident at the LHC.

7 Conclusions

In this paper we have outlined a strategy to discover single-top-quark production via W -gluon fusion and measure its cross section at the Fermilab Tevatron and the CERN LHC. The signal is extracted by searching for a semileptonically-decaying top quark with one b tag, a non- b -tagged jet, and no additional jets or leptons. We have also studied single-top-quark production via $q\bar{q} \rightarrow t\bar{b}$, which can be separated from W -gluon fusion (at the Tevatron) by requiring two b tags. These two single-top-quark production processes provide independent measurements of the CKM matrix element V_{tb} , and are generally influenced by new physics in different ways.

Since the final state in single-top-quark production via W -gluon fusion ($qg \rightarrow t\bar{b}q$) contains a \bar{b} antiquark in addition to the desired signal, we have calculated the cross section with the p_T of the \bar{b} antiquark below 20 GeV. This is a large fraction of the total cross section, since the \bar{b} antiquark arises from the splitting of the initial gluon to a nearly-collinear $b\bar{b}$ pair, and hence is usually at low p_T . The calculation of this cross section requires careful consideration of the collinear region. We obtained this cross section by subtracting the cross section with $p_T > 20$ GeV from the next-to-leading-order total cross section. The resulting cross section, listed in Table 1, has an uncertainty of about $\pm 10\%$ (estimated by varying the scale in the gluon distribution function and the strong coupling), as well as an additional uncertainty of $\pm 10\%$ from the parton distribution functions, resulting in a total theoretical uncertainty of $\pm 15\%$.

The accuracy with which V_{tb} can be extracted from single-top-quark production via W -gluon fusion is listed in Table 4. An accuracy of about $\pm 12\%$ should be achieved in Run II at the Tevatron. The accuracy saturates at 7.6% (half the theoretical uncertainty) at both the Tevatron (30 fb^{-1}) and the LHC. Improving the accuracy therefore requires additional

work to reduce the theoretical uncertainty in the cross section.

We also considered single-top-quark production via $q\bar{q} \rightarrow t\bar{b}$. This process has a smaller theoretical uncertainty, but a larger statistical uncertainty. The accuracy with which V_{tb} can be extracted via this process is listed in Table 6. The accuracy is only slightly worse than that of W -gluon fusion in Run II at the Tevatron. With additional integrated luminosity (30 fb^{-1}), an accuracy of $\pm 5\%$ can be achieved, somewhat better than that of W -gluon fusion. Single-top-quark production via $q\bar{q} \rightarrow t\bar{b}$ is much more difficult to extract at the LHC due to the large background from $t\bar{t}$ and W -gluon fusion.

We also considered the amount of data needed to detect the polarization of the top quark in single-top-quark production via W -gluon fusion. We found that Run II at the Tevatron will produce evidence for this effect. Approximately 5 fb^{-1} of integrated luminosity is needed to establish the polarization at the 5σ level.

Single-top-quark production via W -gluon fusion and $q\bar{q} \rightarrow t\bar{b}$ represents an entirely new window into the weak interactions of the top quark. We eagerly await their discovery in Run II at the Tevatron.

Note added: While completing this work, another paper on single-top-quark production at hadron colliders appeared [47]. This paper advocates using a signal consisting of the decay products of the top quark plus one or two additional jets, with two b tags. This is similar to our s -channel analysis, although we require one and only one additional jet.

Acknowledgements

We are grateful for conversations and correspondence with D. Amidei, R. Frey, C. Hill, T. Liss, F. Paige, S. Parke, M. Seymour, T. Sjostrand, and W.-M. Yao. This work was supported in part by Department of Energy grant DE-FG02-91ER40677. Z. S. was supported in part by a grant from the UIUC Campus Research Board.

References

- [1] S. Willenbrock and D. Dicus, Phys. Rev. D **34**, 155 (1986).
- [2] C.-P. Yuan, Phys. Rev. D **41**, 42 (1990)
- [3] R. K. Ellis and S. Parke, Phys. Rev. D **46**, 3785 (1992).
- [4] D. Carlson and C.-P. Yuan, Phys. Lett. B **306**, 386 (1993).
- [5] A. Heinson, A. Belyaev, and E. Boos, Phys. Rev. D **56**, 3114 (1997).
- [6] S. Cortese and R. Petronzio, Phys. Lett. B **253**, 494 (1991).
- [7] T. Stelzer and S. Willenbrock Phys. Lett. B **357**, 125 (1995).
- [8] D. Carlson, E. Malkawi, and C.-P. Yuan, Phys. Lett. B **337**, 145 (1994).
- [9] D. Atwood, S. Bar-Shalom, G. Eilam, and A. Soni, Phys. Rev. D **54**, 5412 (1996).
- [10] A. Datta and X. Zhang, Phys. Rev. D **55**, 2530 (1997).
- [11] C. S. Li, R. Oakes, and J. M. Yang, Phys. Rev. D **55**, 1672 (1997); **55**, 5780 (1997).
- [12] E. Simmons, Phys. Rev. D **55**, 5494 (1997).
- [13] G. Lu Y. Cao, J. Huang, J. Zhang, and Z. Xiao, hep-ph/9701406.
- [14] A. Datta, J. Yang, B.-L. Young, and X. Zhang, Phys. Rev. D **56**, 3107 (1997).
- [15] T. Tait and C.-P. Yuan, hep-ph/9710372.
- [16] M. Dittmar, F. Pauss, and D. Zürcher, Phys. Rev. D **56**, 7284 (1997).
- [17] M. Smith and S. Willenbrock Phys. Rev. D **54**, 6696 (1996).
- [18] *Report of the tev_2000 Study Group*, edited by D. Amidei and R. Brock, Fermilab-Pub-96/082 (1996).
- [19] G. Bordes and B. van Eijk, Nucl. Phys. **B435**, 23 (1995).

- [20] T. Stelzer, Z. Sullivan, and S. Willenbrock, Phys. Rev. D **56**, 5919 (1997).
- [21] S. Moretti, Phys. Rev. D **56**, 7427 (1997).
- [22] W. Giele, S. Keller, and E. Laenen, Phys. Lett. B **372**, 141 (1996).
- [23] G. Mahlon and S. Parke, Phys. Rev. D **55**, 7249 (1997).
- [24] J. Huston, S. Kuhlmann, H. Lai, F. Olness, J. Owens, D. Soper, and W.-K. Tung, hep-ph/9801444.
- [25] S. Blusk, presented at the XXXIII Rencontres de Moriond on QCD and High Energy Hadronic Interactions, Les Arcs, France, March 21-28, 1998 (hep-ex/9805035).
- [26] A. Stange, W. Marciano, and S. Willenbrock, Phys. Rev. D **49**, 1354 (1994); **50**, 4491 (1994).
- [27] T. Stelzer and W. F. Long, Comp. Phys. Comm. **81**, 357 (1994).
- [28] P. Nason, S. Dawson and R. K. Ellis, Nucl. Phys. **B303**, 607 (1988); **B327**, 49 (1989); Erratum **B335**, 260 (1990).
- [29] W. Beenakker, H. Kuijf, W. van Neerven, and J. Smith, Phys. Rev. D **40**, 54 (1989); R. Meng, G. Schuler, J. Smith, and W. van Neerven, Nucl. Phys. **B339**, 325 (1990); W. Beenakker, W. van Neerven, R. Meng, G. Schuler, and J. Smith, Nucl. Phys. **B351**, 507 (1991).
- [30] S. Catani, M. Mangano, P. Nason, L. Trentadue, Phys. Lett. B **378**, 329 (1996); Nucl. Phys. **B478**, 273 (1996); hep-ph/9801375.
- [31] E. Laenen, J. Smith, and W. van Neerven, Nucl. Phys. **B369**, 543 (1992).
- [32] E. Berger and H. Contopanagos, Phys. Lett. B **361**, 115 (1995); Phys. Rev. D **54**, 3085 (1996); **57**, 253 (1998).

- [33] F. Olness and W.-K. Tung, Nucl. Phys. **B308**, 813 (1988); M. Aivazis, J. Collins, F. Olness, and W.-K. Tung, Phys. Rev. D **50**, 3102 (1994).
- [34] R. Barnett, H. Haber, and D. Soper, Nucl. Phys. **B306**, 697 (1988).
- [35] C.-P. Yuan, in *6th Mexican School of Particles and Fields*, edited by J. D’Olivo, M. Moreno, and M. Perez (World Scientific, Singapore, 1995), p. 16; D. Carlson, hep-ph/9508278.
- [36] CTEQ Collaboration, H. Lai *et al.*, Phys. Rev. D **55**, 1280 (1997).
- [37] W.-M. Yao, in *Proceedings of the 1996 DPF/DPB Summer Study on New Directions for High-Energy Physics*, Snowmass, eds. D. Cassel, L. Gennari, and R. Siemann (SLAC, Menlo Park, 1997), p. 619.
- [38] ATLAS Technical Proposal, CERN/LHCC/94-43, p. 98.
- [39] V. Barger, K. Cheung, T. Han, and D. Zeppenfeld, Phys. Rev. D **44**, 2701 (1991); Erratum **48**, 5444 (1993).
- [40] SLD Collaboration, K. Abe *et al.*, Phys. Rev. Lett. **80**, 660 (1998).
- [41] SLD Collaboration, presented at the International Europhysics Conference on High Energy Physics, Aug. 19-26, Jerusalem, SLAC-PUB-7585 (1997).
- [42] R. Kleiss and W. J. Stirling, Phys. Lett. B **200**, 193 (1988); R. Cahn, S. Ellis, R. Kleiss, and W. J. Stirling, Phys. Rev. D **35**, 1626 (1987).
- [43] V. Barger, T. Han, and R. Phillips, Phys. Rev. D **37**, 2005 (1988).
- [44] U. Baur and E. W. N. Glover, Phys. Lett. B **252**, 683 (1990); Nucl. Phys. **B347**, 12 (1990).
- [45] I. Bigi, Y. Dokshitzer, V. Khoze, J. Kühn, and P. Zerwas, Phys. Lett. B **181**, 157 (1986).
- [46] M. Jezabek, Nucl. Phys. B (Proc. Suppl.) **37B**, 197 (1994).

[47] A. Belyaev, E. Boos, and L. Dudko, hep-ph/9806332.